

PAPER • OPEN ACCESS

Research on Electron Evolution of Atmospheric Pressure Pulsed Dielectric Barrier Discharge Based on Two-dimensional Symmetrical Fluid Model

To cite this article: Xingyu Chen *et al* 2021 *J. Phys.: Conf. Ser.* **2030** 012017

View the [article online](#) for updates and enhancements.

You may also like

- [A homogeneous dielectric barrier discharge plasma excited by a bipolar nanosecond pulse in nitrogen and air](#)
De-Zheng Yang, Yang Yang, Shou-Zhe Li et al.
- [Performance and optimum characteristics by finite element analysis of a coreless ironless electric generator for low wind density power generation](#)
Akhtar Razali, Fadhur Rahman, Yap Wee Leong et al.
- [Computational simulation of platelet interactions in the initiation of stent thrombosis due to stent malapposition](#)
Jennifer K W Chesnutt and Hai-Chao Han



IOP | ebooks™

Bringing together innovative digital publishing with leading authors from the global scientific community.

Start exploring the collection—download the first chapter of every title for free.

Research on Electron Evolution of Atmospheric Pressure Pulsed Dielectric Barrier Discharge Based on Two-dimensional Symmetrical Fluid Model

Xingyu Chen, Chen Lu, Zilan Xiong *

State Key Laboratory of Advanced Electromagnetic Engineering and Technology, Huazhong University of Science and Technology, WuHan, Hubei 430074, People's Republic of China

*Corresponding author's e-mail: zilanxiong@hust.edu.cn

Abstract. In recent years, plasma technology under atmospheric pressure has been widely used, and it is urgent to study the mechanism of plasma microcosmic particles. With the development of computer technology, it may be a promising method to describe the microcosmic discharge process by simulation. In this study, a two-dimensional symmetrical fluid model of ns pulse dielectric barrier discharge (DBD) at atmospheric pressure was constructed using COMSOL software. The movement behavior of electrons in different working gas, different gap distance and different electrode radius was analyzed. It was found that in helium, the electrons would move to the outside electrode area with low electron density obviously. In argon, the electrons would always be mainly constrained within the electrode area, and the electron density is more than 10^5 times than that of the initial value. Changing the gap distance will change the diffusion rate and maximum density of electrons. The electron distribution will be more homogeneous, and the density within the electrode area will increase 10^2 - 10^3 times at large gap distance. Changing the electrode diameter has little impact on electron movement behavior. The validity of the model is verified by comparing experimental and simulated voltage and current waveforms.

1. Introduction

With the wide application of low temperature plasmas in various fields, the generation of uniform low-temperature plasmas at atmospheric pressure has become one of the research hotspots worldwide. [1-2] Dielectric barrier discharge (DBD) is one of the main plasma source to generate large uniform plasmas. With the development of pulse power technology, pulsed DBD with repetitive pulse voltage as the excitation power source shows its unique advantages. [3-5] Pulsed DBD under atmospheric pressure has a wide range of applications in material modification, sterilization, environmental treatment and so on. Compared with the traditional AC DBD, the ultra-fast rising and falling edge in the pulse discharge process can produce quick ionizing wave and higher electron energy. It is an energy-saving and efficient treatment method, which is getting more and more attention. [6-7] Pulsed DBD has different discharging morphologies in different electrode structures and working gases. Pulsed DBD discharge in helium and argon is easier to realize uniform discharge, which is a kind of low-cost treatment method of materials. [8-10].

In recent years, Laroussi et al. [11] used nanosecond pulse drive to generate uniform DBD plasma under atmospheric pressure in He, and measured the electron density of the discharge at the same time. The measurement results showed that the electron density under the nanosecond pulse-driven was as



Content from this work may be used under the terms of the [Creative Commons Attribution 3.0 licence](https://creativecommons.org/licenses/by/3.0/). Any further distribution of this work must maintain attribution to the author(s) and the title of the work, journal citation and DOI.

high as $8 \times 10^{12} \text{cm}^{-3}$, which was several times higher than that of the traditional AC-driven DBD plasma. Sergey O [12] used a fluid model to study pulsed DBD. It was found that the method of fluid simulation can accurately calculate macroscopic parameters such as voltage, current, and microscopic parameters such as electrons density. However, although many experts and scholars have done some related work for atmospheric pressure pulsed DBD, there are still many issues need to be solved. For example, the mechanism of pulsed DBD under atmospheric pressure is not fully understood yet, and the relationship between macroscopic parameters and microscopic processes is not clear.

The simulation for the discharge process mainly includes the fluid model and the particle model. The fluid model treats the plasma as the cluster of charged gas and analyzes it through the overall equations, so the calculation speed is faster. The particle model simulates all particles in the simulated area with high accuracy, but its calculated time is longer. In this paper, a two-dimensional symmetry fluid model is used to simulate the discharge process based on the basic particle diffusion equations.

The distribution of electrons in pulsed DBD has direct correlation with macroscopic discharge morphology. In previous simulation studies, the simplified one-dimensional model is mainly used, which is difficult to reflect the distribution of particles in different places of the gas gap. This paper establishes a two-dimensional COMSOL symmetry fluid model to simulate the electron evolution process under atmospheric pressure in different electrode diameters and gap distance in pulsed He/Ar DBD. The movement behavior and the density of electrons in different gas environment is presented, and the main factors affecting the distribution of electrons under pulse DBD are analyzed. The validity of the model is verified by comparing experiments and simulated voltage and current waveforms.

2. Process of experiment and simulation

2.1. Experimental setup

The schematic diagram of the experimental setup of pulsed DBD used in this investigation is shown in Figure 1. The experimental platform consists of a high-voltage pulse power supply, a DBD device, gas channels and measurement system. The high-voltage DC power supply (SPELLMAN-SL300), signal generator (TEKtronix-AFG31000) and pulse amplifier (DEI-PVX-4110) jointly generates high-voltage pulse signals. The voltage amplitude, frequency and the pulse width was fixed at 5kV, 8kHz and 5 μ s, respectively. Both the rising and falling edge of the applied pulse were 50ns. The voltage and current were measured by a high-voltage probe (TEKtronix-P6015A) and a current probe (PEARSON-6585), respectively. The feeding gas was injected into the reaction chamber through a mass flow controller. The working gas was pure helium or argon, and the gas flow rate was 2L/min. The DBD device is a traditional parallel plate electrode structure, which will be described in detail in the next section.

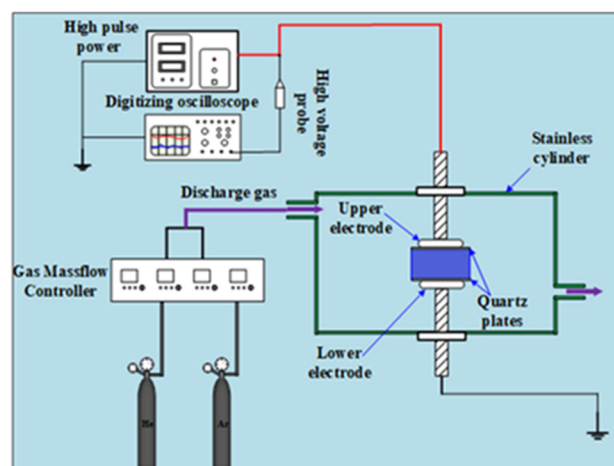


Figure 1. Experimental setup.

2.2. Theoretical formula simulation structure

The DBD device uses copper electrodes with a radius of 7.5mm/20mm. Both of the electrodes are covered with quartz plates. The quartz plate has a radius of 25mm and a thickness of 1.2mm. The gas gap is 2mm/4mm. The electrode and dielectric plate are cylindrically symmetric, and a two-dimensional symmetrical fluid model was used for modeling. The model structure is shown in Figure 2. The simulated results presented the first 10 μ s of the pulse period. During the discharge, the rising edge, the flat-top, and falling edge were all included.

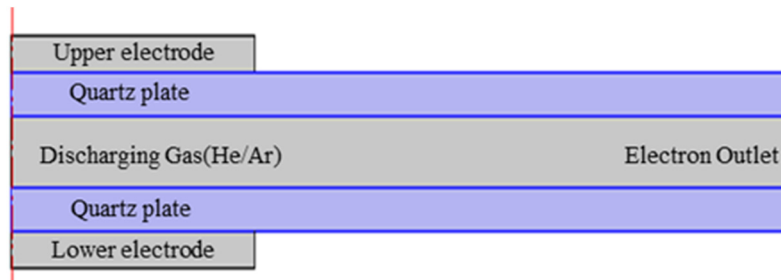


Figure 2. COMSOL model diagram of pulsed DBD

The initial density of the electron n_{e0} is $10^{13}/\text{m}^3$ and the initial speed of μ is 0. The relation between electron concentration and time satisfies the convection-diffusion equation:

$$\frac{\partial n_e}{\partial t} + \Delta \cdot \Gamma_e = R_e - (\mu \cdot \nabla) n_e \quad (1)$$

Γ_e is the electron energy flux, which is used to obtain the spatial distribution of the electron energy. The electron energy mobility and the electron energy diffusion rate are the functions of the average electron energy, which are calculated according to the electron collision cross-section data. The solution equation is as follows: energy, which are calculated according to the electron collision cross-section data. The solution equation is as follows:

$$\Gamma_e = -(\mu_e \cdot E) n_e - D_e \cdot \nabla n_e \quad (2)$$

μ_e is the electronic mobility with a value of $0.1131 \text{m}^2/(\text{v}\cdot\text{s})$.

There is a large amount of charges on the surface of the quartz plate, the calculation of charges and electric field are based on the Poisson equations:

$$E = -\nabla V \quad (3)$$

$$\nabla \cdot (\epsilon_0 \epsilon_r E) = \rho_q \quad (4)$$

ϵ_0 is the permittivity of vacuum, $\epsilon_0 = 8.854 \times 10^{-12} \text{F/m}$. ϵ_r is the relative permittivity. The relative permittivity of the quartz plate is 3.7.

The accumulation of charge eventually leads to the discharge, and the surface current density satisfies the equation:

$$\frac{\partial \rho_s}{\partial t} = n \cdot J_e + n \cdot J_i \quad (5)$$

Where J_i is the ion current density and J_e is the electronic current density.

The discharged gas is He/Ar with a single composition, and only He^* & $\text{He}^{+/}$ & Ar^* & Ar^{+} are considered as product. Particle reaction, and rate of reaction are shown in Table 1

Table 1. The chemical reaction formula involved of He and Ar in ns pulse DBD

Reaction equation	Rate Coefficient(cm^3s^{-1})	Reference
$e + \text{He} \rightarrow \text{He}^* + e$	$4.2 \times 10^{-9} T_e^{0.31} \exp(-19.8/T_e)$	[13]
$e + \text{He}^* \rightarrow \text{He} + e$	2.9×10^{-9}	[14]
$e + \text{He} \rightarrow \text{He}^+ + 2e$	$1.5 \times 10^{-9} T_e^{0.68} \exp(-24.6/T_e)$	[13]
$e + \text{He}^* \rightarrow \text{He}^+ + 2e$	$1.28 \times 10^{-7} T_e^{0.6} \exp(-4.78/T_e)$	[13]
$\text{He}^* + \text{He}^* \rightarrow \text{He}^+ + e + \text{He}$	2.7×10^{-10}	[13]

$e+\text{He}^+\rightarrow\text{He}$	$1.327n_e\times 10^{-21}(T_e/T_g)^{-0.44}$	[13]
$e+\text{Ar}\rightarrow\text{Ar}^+e$	$2.5\times 10^{-9}T_e^{0.74}\exp(-11.56/T_e)$	[15]
$e+\text{Ar}^*\rightarrow\text{Ar}+e$	$4.3\times 10^{-10}T_e^{0.74}$	[15]
$e+\text{Ar}\rightarrow\text{Ar}^++2e$	$2.3\times 10^{-8}T_e^{0.68}\exp(-15.76/T_e)$	[15]
$e+\text{Ar}^*\rightarrow\text{Ar}^++2e$	$6.8\times 10^{-9}T_e^{0.67}\exp(-4.2/T_e)$	[15]
$\text{Ar}+\text{Ar}^*\rightarrow\text{Ar}+\text{Ar}$	5.53×10^{-7}	[15]
$\text{Ar}^*+\text{Ar}^*\rightarrow\text{Ar}+e+\text{Ar}^+$	3.02×10^{-12}	[15]

* T_e is the electron temperature.

3. Results and discussions

3.1. Comparison of experimental and simulated voltage and current waveforms

By controlling other variables unchanged, the influence of one variable on the evolution of electrons can be obtained intuitively. From equation (1)-equation (5), the electron density distribution in the gap under different voltages can be obtained. It is also possible to obtain the total discharge current on the electrode surface and compare it with the experimental voltage and current waveforms. Taking the 7.5mm electrode radius and the 2mm gap distance condition as an example, the experimental and simulated voltage and current diagrams in He and Ar are shown in Figure 3. A positive current pulse is formed at the rising edge of the pulse, and a negative current pulse is formed at the falling edge. The maximum value of the rising edge current in He is $\sim 2\text{A}$, and in Ar it is only 0.5A. The waveforms and amplitudes of the simulation and experiment are consistent, indicating that it is feasible to simulate the pulsed DBD process by this model.

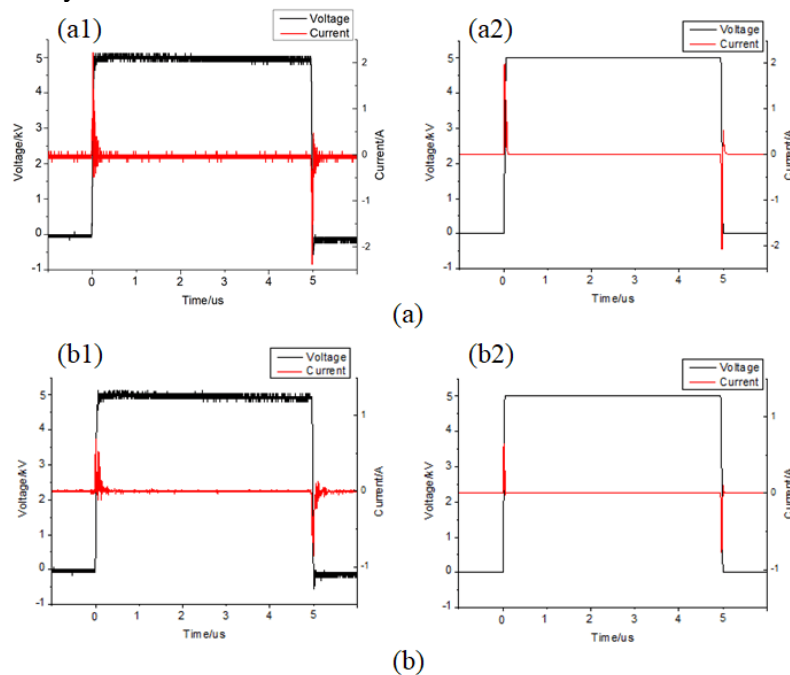


Figure 3. Experimental and simulated voltage and current waveforms under 7.5mm radius electrode and 2mm gap (a) in He, (a1) experimental, (a2) simulated; (b) in Ar, (b1) experimental, (a2) simulated.

3.2. The influence of working gas and gap distance on discharge morphology and electron behavior

Working gas is one of the main factors that affects the evolution of electrons. Although both He and Ar are rare gases and exist in the form of monoatomic molecules, their particle reactions are similar, however, the discharge evolution is different. During the rising edge in helium discharge, electrons quickly gather to the anode, and the electron density inside the electrode area decreases to 10^{-3} times

that of the initial time. In argon, the electron density inside the electrode area remains high, which is 10^5 times than that of the initial time. The results are shown in Figure 4(a) and Figure 4(b). In Fig. 4(a), in the first $0.05\mu\text{s}$, that is, the rising edge of the pulse voltage, electrons are gathered on the anode, and the current reached the maximum value. During $0.05\mu\text{s}$ - $0.1\mu\text{s}$, the voltage is stable, the electrons starts to diffuse rapidly to the outside of the electrode area. In Figure 4(b), the electrons are basically confined within the electrode area after $0.05\mu\text{s}$. The main reasons are the following two points: As can be seen from Table 1, the recombination reaction rate of He^+ ions in helium is relatively high and can't be ignored. This means that the electrons inside the electrode and He^+ will recombine at a certain concentration or a large amount of recombination when discharging in helium. The electron density is difficult to further increase, and the probability of recombination reaction in argon gas is greatly reduced, so that the consumption of electrons is greater than generation. After broken down in He, the particles are subjected to the longitudinal force of the electrode. The electron density of the discharge area inside the electrode is lower than the initial value, which plays the important role of discharge maintain. The electron density on the outside of the electrode is also reduced, and the overall movement escapes to the outside of the electrode, because the lateral repulsive force of the remaining particles can't be ignored. Under the same discharge conditions, for the argon atoms are heavier, the positive ions distribution is more concentrated. After broken down, the particles are mainly subjected to the longitudinal force of the electrode, and the lateral repulsive force of the remaining particles can be neglected.

When other conditions remain unchanged, the larger the gap distance, the more difficult for the gas to break down. The evolution process in 4mm gas gap is shown in Figure 5. Comparing Fig. 4(a) and Fig. 5(a) in He discharge, electrons have gathered to the anode and began to diffuse outward under the 2mm gas gap at $0.1\mu\text{s}$, while the electrons under the 4mm gas gap are still moving towards the anode. The electron density under the 4mm gap is up to $10^{15}/\text{m}^3$, which is about 100 times higher than that under the 2mm gap. Comparing Fig. 4(b) with Fig. 5(b), when the working gas is argon, electrons accumulate to the anode and remain stable under the condition of 2mm gas gap at $0.05\mu\text{s}$, while under 4mm gas gap will not be until $0.1\mu\text{s}$. The maximum electron density under the 4mm gap reaches $10^{20}/\text{m}^3$, which is about 1000 times of that under the 2mm gap. During the rising edge, the electrons will be assembled more quickly under the 2mm gap, but the maximum electron density is only 10^{-3} - 10^{-2} times of that under the 4mm gap. The reason is that the electric field strength is larger when the gap is small, and the distance between the electrons moving to the anode is shorter, so the electrons accumulate in the positive electrode dielectric much faster, the total number of electrons in the space is less.

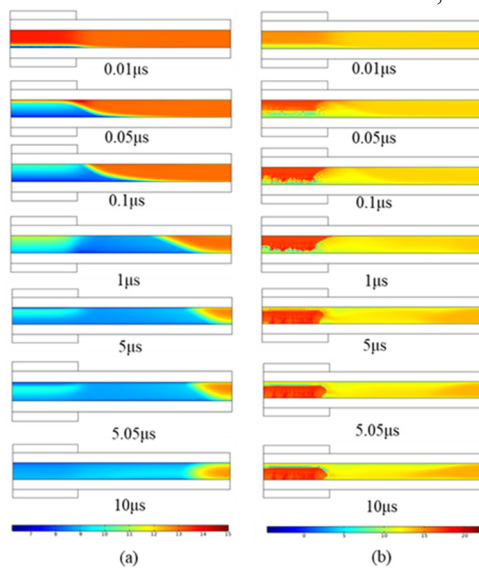


Figure 4. Electron distribution evolution diagram under 7.5mm radius electrode and 2mm gap (a)He (b)Ar.

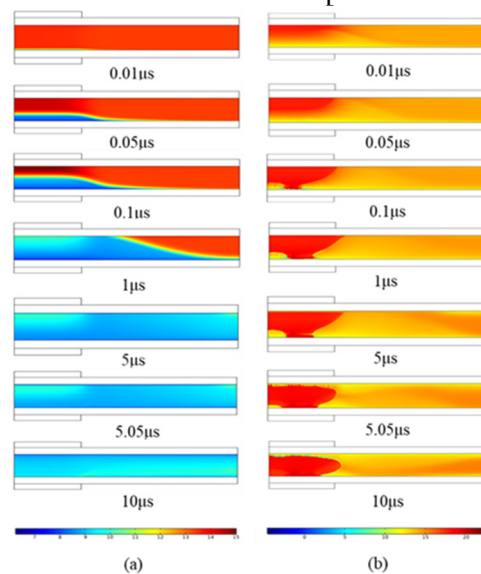


Figure 5. Electron distribution evolution diagram under 7.5mm radius electrode and 4mm gap (a)He (b)Ar.

3.3. The impact of the electrode diameter

The evolution process of electrons under the large electrode with a radius of 20mm is shown in Figure 6 and Figure 7. Comparing the graphs (a) and (b) of these two figures, and comparing the results with Fig. 4 and Fig. 5, it is found that the discharge differences in different working gases and different gap distances are consistent with the analysis in the previous section. That is, when the working gas is helium, the electrons will expand after the rising edge ends. When the working gas is argon, the electrons are mainly bounded within the electrode area. Increasing the gas gap will make the electrons move more slowly, but it also can increase the maximum electron density. However, when the electrode radius is changed, the electron evolution process does not change significantly.

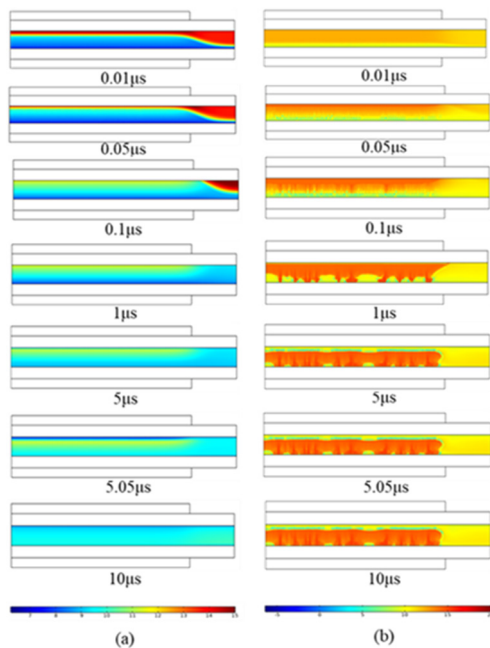


Figure 6. Electron distribution evolution diagram under 20mm radius electrode and 2mm gap (a)He (b)Ar.

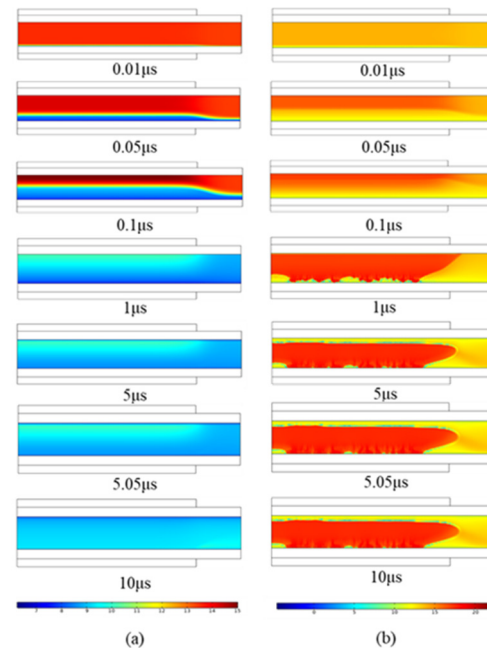


Figure 7. Electron distribution evolution diagram under 20mm radius electrode and 4mm gap (a)He (b)Ar.

4. Conclusions

A 2D symmetrical fluid model was built up to monitor the electron behavior in pulse DBD at atmospheric pressure, this contributes to the study of microcosmic discharge process and the precise control of discharge area. The consistency of the experimental and simulated voltage and current during both He/Ar discharge verified the reliability of the model.

Working gas is one of the main factors that affects the discharge pattern and electron behavior. In He discharge, the electron density after break down is low, which is only 10^{-3} times that of the initial time, and the electrons diffuse to the outside of the electrode after certain time. However, in argon discharge, the electrons mainly gather inside the electrode area with electron density 10^5 times higher than that of the initial time.

Changing the gap distance will also affect the electron evolution. The motion tendency in He/Ar is similar under 2mm and 4mm gap, but the highest electron density of 2mm gap in helium and argon are only 10^{-3} - 10^{-2} times of that in 4mm gap. Meanwhile, the size of the electrode does not affect the electron distribution results.

In the future, more physical quantities such as discharge parameters can be changed to further study the factors affecting the discharge process.

References

- [1] Philip D., Gill M., Cliff S., Andrew J., Watson., Peter S., Robert C. (2000) In situ evaluation of air-sea gas exchange parameterizations using novel conservative and volatile tracers. *J. Global Biogeochemical Cycles*, 14(1):373-387.
- [2] Lu X P., Ye T., Cao Y G., et al. (2008) The roles of the various plasma agents in the inactivation of bacteria. *J. Journal of Applied Physics*, 104(5):1632.
- [3] Lee K., Paek K H., Ju W T., et al. (2006) Sterilization of Bacteria, Yeast, and Bacterial Endospores by Atmospheric-Pressure Cold Plasma using Helium and Oxygen. *J. The Journal of Microbiology*, 44(3):269-275.
- [4] Kim B., Yun H., Jung S. (2011) Effect of atmospheric pressure plasma on inactivation of pathogens inoculated onto bacon using two different gas compositions. *J. Food Microbiology*, 28(1):9-13.
- [5] Yuan, L., Wang L., Ma K., Guo L., Xing X. H. (2011) Characteristics of Hydrogen Production of an *Enterobacter aerogenes* Mutant Generated by a New Atmospheric and Room Temperature Plasma (ARTP). *J. Biochemical Engineering Journal*, 55(1):17-22.
- [6] Brandenburg R. (2017) Dielectric Barrier Discharges: Progress on Plasma Sources and on the Understanding of Regimes and Single Filaments. *J. Plasma Sources Science and Technology*, 26(5).
- [7] Tao S., Kaihua L., Cheng Z. (2008) Experimental study on repetitive unipolar nanosecond-pulse dielectric barrier discharge in air at atmospheric pressure. *J. Journal of Physics D Applied Physics*, 41(21):215203.
- [8] Obradovi B M., Sretenovi G B., Kuraica M M. (2006) A dual-use of DBD plasma for simultaneous NO_x and SO₂ removal from coal-combustion flue gas. *J. Journal of Hazardous Materials*, 185(2-3):1280-1286.
- [9] Claire Tenderoa A., Christelle Tixiera A., Pascal Tristanta A. (2005) Atmospheric pressure plasmas: A review – ScienceDirect. *J. Spectrochimica Acta Part B: Atomic Spectroscopy*, 61(1):2-30.
- [10] Gibalov V I., Pietsch G J. (2000) The development of dielectric barrier discharges in gas gaps and on surfaces. *J. Journal of Physics D Applied Physics*, 33(20), 2618.
- [11] Laroussi M., Lu X., Kolobov V., et al. (2004) Power consideration in the pulsed dielectric barrier discharge at atmospheric pressure. *J. Journal of Applied Physics*, 96(5):3028-3030.
- [12] Macheret S O., Shneider M N., Miles R B. (2002) Modeling of air plasma generation by repetitive high-voltage nanosecond pulses. *J. IEEE Transactions on Plasma Science*, 30(3):1301-1314.
- [13] Carman., Robert, J. (2002) Computer modeling of electrical breakdown in a pulsed dielectric barrier discharge in xenon. *J. IEEE Transactions on Plasma Science*, 30(1), 154-155.
- [14] Park G., Lee H., Kim G. (2008). Global model of He/O and Ar/O atmospheric pressure glow discharges. *J. Plasma Processes & Polymers*, 5(6), 569-576.
- [15] Lee, M.H., Chung C.W. (2005) Self-consistent global model with multi-step ionizations in inductively coupled plasmas. *J. Physics of Plasmas*, 12(7), 073501-073501-5.